ACTA CHEMICA SCANDINAVICA 26 (1972) 3215–3225

^{121}Sb Mössbauer Studies on Compounds with Pyrite, Marcasite, and Arsenopyrite Type Structures

J. D. DONALDSON,[a] A. KJEKSHUS,[b] D. G. NICHOLSON[b] and M. J. TRICKER[a]

[a] *Department of Chemistry, Chelsea College of Science and Technology, Manresa Road, London S.W.3, England and* [b] *Department of Chemistry, University of Oslo, Blindern, Oslo 3, Norway*

^{121}Sb Mössbauer parameters for $CrSb_2$, $FeSb_2$, $CoSb_2$, $NiSb_2$, $RuSb_2$, $RhSb_2$, $OsSb_2$, $IrSb_2$, $PtSb_2$, and $AuSb_2$ are reported and discussed in relation to the pyrite, marcasite, and arsenopyrite type structures. At 4.2 K the chemical shifts fall within the range -11.1 to -8.5 mm/s with respect to $Ba^{121}SnO_3$ and the quadrupole coupling constants vary between 2.7 and 14.8 mm/s, V_{zz} being negative in all cases. The data are consistent with these compounds having a predominantly covalent type of bonding, and there is a correlation between the quadrupole coupling constant and the average angular distortion from tetrahedral symmetry around the Sb sites.

The present work forms an integral part of an "ambitious" research programme on TX_2 compounds with the pyrite (FeS_2-*p*), marcasite (FeS_2-*m*), and arsenopyrite (FeAsS; binary prototype $CoSb_2$) type crystal structures. The previous endeavour has *inter alia* led to a bonding scheme which ascribes essentially pure σ-character to the $T-X$ ($,T-T,$) and $X-X$ bonds in these compounds.[1,2] The consequent lack of a significant contribution from π back-bonding between the metal (T) and non-metal (X) atoms has been given support by an analysis of the bonding interatomic distances and the ^{57}Fe Mössbauer parameters.[3] Most of the experimental evidence in this field focuses attention on the metal atoms and their immediate environment, whereas, except for crystal structure data, very little decisive information is available concerning the non-metal atoms. However, Mössbauer methodology is now sufficiently advanced to permit a study on compounds containing ^{121}Sb. This paper is devoted to an examination of the ^{121}Sb Mössbauer parameters in $CrSb_2$, $FeSb_2$, $CoSb_2$, $NiSb_2$, $RuSb_2$, $RhSb_2$, $PdSb_2$, $OsSb_2$, $IrSb_2$, $PtSb_2$, and $AuSb_2$, which belong to one or another of the three structure types concerned. Data for $PdSb_2$ are already available through the work of Montgomery and Ruby.[4]

Some of the questions which emerge on shifting attention from the metal to the non-metal atoms are:

(i) Are there any correlations between the ^{121}Sb Mössbauer parameters and the respective structure types? This question arises because the degree of distortion of the tetrahedral configuration of one X and three T atoms bonded to each X is one consequence of the structure type. The term structure type is hence employed in its broadest sense to encompass the classes A, A/B, and B of the marcasites, *cf.* Refs. 1,2. A particular point of interest for the compounds with the $CoSb_2$ type structure is whether the two crystallographically non-equivalent Sb sites are reflected in their ^{121}Sb Mössbauer spectra.

(ii) Are the ^{121}Sb Mössbauer parameters directly related to the configuration (d^j) of the essentially non-bonding electrons which are localized on the T atoms? Any such measurable relationship may be caused by the differences in the bonding characteristics (*viz.* bond strength, *cf.* Ref. 3) associated with the d^j configurations and spin states of the metal atoms. This effect comes in addition to that which originates from the fact that the structure type is, in part, governed by the d^j configuration on T (see i above), although it is clearly difficult to separate the two contributions.

(iii) $CrSb_2$ undergoes a transition to an antiferromagnetic state at a Néel temperature of 273 ± 2 K.[5] The life-time of the ^{121}Sb Mössbauer state is short and a large magnetic field at the Sb nucleus is necessary in order for it to be resolvable. Are we able to observe the effects of magnetic splitting at any temperature?

(iv) Are the ^{121}Sb Mössbauer parameters in accordance with the other experimental data at hand for these compounds? This is of particular importance because most of the information is consistent with the current bonding model.[1–3]

EXPERIMENTAL

The samples were prepared as described in preceding papers [6–8] and their homogeneities were ascertained from Guinier photographic X-ray data. Only samples with the stoichiometric 1:2 composition were utilized in the present study.

The samples were finely powdered and dispersed in grease before pressing between two layers of aluminium foil. In this way suitable Mössbauer absorbers were obtained with a thickness of ~ 10 mg Sb per absorber area.

Both the absorbers and source (1 mCi $Ba^{121}SnO_3$) were kept at liquid nitrogen or liquid helium temperature. The source motion was provided by a moving coil drive system linked to a Laben analyser operating in the multiscaler mode. Approximately 10^5 counts were collected per channel in each spectrum. The 37.2 keV γ-radiation was detected with a Xe/CH_4 proportional counter, the analyser window being set on the 6 keV escape peak. Calibrations were performed before and after each experiment. The liquid helium data were collected at the P.C.M.U., Harwell, U.K.

The short half-life of the excited state of the $7/2 \rightarrow 5/2$ Mössbauer transition of ^{121}Sb usually results in unresolved eight-line quadrupole split spectra. The data were reduced by a computer programme which performed a least squares fit to a series of absorption peaks having Lorentzian shapes on a parabolic base line. The individual peak positions and intensities were calculated assuming axially symmetric quadrupole interaction and were constrained in the ratios expected according to the quadrupole Hamiltonians and the Clebsh Gordon coefficients. The ratio of the quadrupole moments of the ground and excited states was taken as 1.34.[9] The following parameters were refined: the scale factor, three parameters defining the parabolic base line, an overall peak half-width for each Lorentzian, the chemical shift (δ), and one quadrupole splitting parameter (eQV_{zz}).

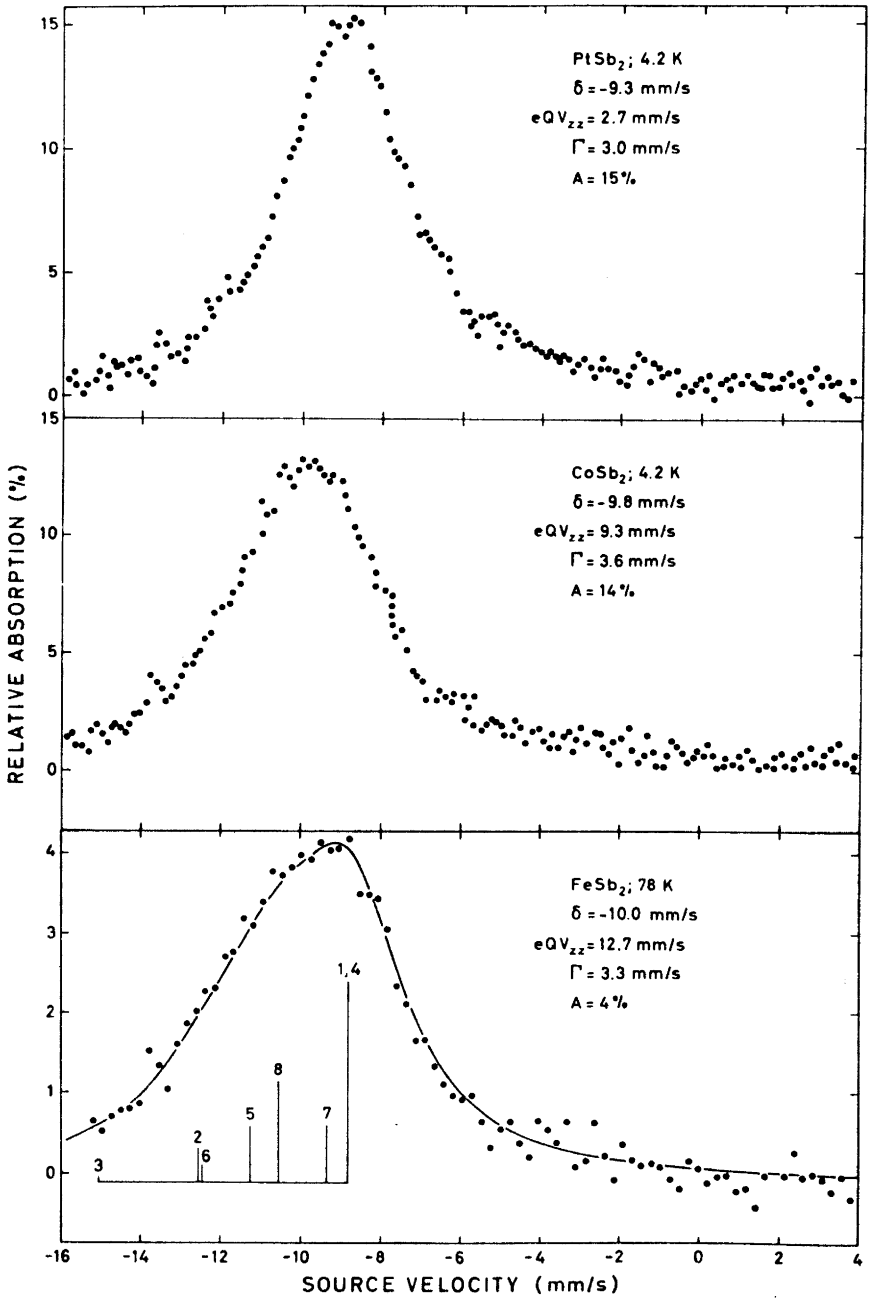

Fig. 1. ^{121}Sb Mössbauer spectra for $FeSb_2$ (78 K), $CoSb_2$ (4.2 K), and $PtSb_2$ (4.2 K).

RESULTS AND DISCUSSION

Fig. 1 shows the ^{121}Sb Mössbauer spectra of $FeSb_2$, $CoSb_2$, and $PtSb_2$ which are representative of the three structure types considered in this study. The $FeSb_2$ spectrum is included as an example of the data obtained at 78 K. Furthermore it serves as a typical example of the generally good agreement obtained between the experimental points and the calculated curve profile. The bar diagram gives the positions of the individual Lorentzians from which the chemical shift (δ) and quadrupole splitting (eQV_{zz}) parameters are extracted. The value of η was constrained to zero in accordance with the virtual C_{3v} symmetry of the Sb sites in these structures (*vide infra*). The numbers attached to the bars identify the individual (allowed) transitions according to convention. The values of δ and eQV_{zz} for all compounds, as derived from the computer analyses, are contained in Table 1. In order to facilitate com-

Table 1. ^{121}Sb Mössbauer parameters for compounds with FeS_2-*p*, FeS_2-*m*, and $CoSb_2$ type structures. Chemical shifts are given with respect to $Ba^{121}SnO_3$.

Compound	Structure type	T (K)	δ^a (mm/s)	eQV_{zz} [b] (mm/s)	Γ^c (mm/s)	A[d] (%)
$CrSb_2$	FeS_2-*m*	4.2	Cannot be fitted			
$CrSb_2$	FeS_2-*m*	78	−9.4	11.3	5.0	7
$FeSb_2$	FeS_2-*m*	4.2	−10.0	14.8	4.7	11
$FeSb_2$	FeS_2-*m*	78	−10.0	12.7	3.3	5
$CoSb_2$	$CoSb_2$	4.2	−9.8	9.3	3.6	14
$CoSb_2$	$CoSb_2$	78	−9.4	8.5	3.0	5
$NiSb_2$	FeS_2-*m*	4.2	−10.0	5.0	3.2	15
$NiSb_2$	FeS_2-*m*	78	−10.2	8.4	3.6	5
$RuSb_2$	FeS_2-*m*	4.2	−9.3	12.4	2.9	14
$RhSb_2$	$CoSb_2$	4.2	−9.1	10.2	4.0	15
$PdSb_2$ [e]	FeS_2-*p*	78	−10.2	4.3	5.6	–
$OsSb_2$	FeS_2-*m*	4.2	−8.9	13.1	3.7	18
$IrSb_2$	$CoSb_2$	4.2	−8.5	7.6	3.7	16
$PtSb_2$	FeS_2-*p*	4.2	−9.3	2.7	3.0	15
$AuSb_2$	FeS_2-*p*	4.2	−11.1	3.0	3.0	12

[a] Probable error ±0.1 mm/s. [b] Probable error ±1 mm/s. [c] Full width at half height. [d] Maximum absorption effect. [e] Quoted from Montgomery and Ruby.[4]

parison with other ^{121}Sb Mössbauer studies it should be recorded that the δ values for InSb are −9.0 and −8.5 mm/s at 4.2 and 78 K, respectively, in satisfactory agreement with those obtained in earlier studies (*cf.*, *e.g.*, Ref. 10). The parameters for $PdSb_2$ are those reported by Montgomery and Ruby.[4]

Before discussing the ^{121}Sb Mössbauer data it is considered profitable to recapitulate on the structural characteristics and bonding information which are at hand [1–3] for the compounds. The following features are common to all of them:

(i) composition TSb$_2$,
(ii) octahedral coordination of 6 Sb atoms around each T atom,
(iii) tetrahedral coordination of 1 Sb and 3 T atoms around each Sb atom, and,
(iv) Sb – Sb pairs.

It should be noted that regular octahedral and tetrahedral symmetries are impossible to realize within this framework.[1] Thus, a more accurate description of the environments of the Sb atoms in the FeS$_2$-p type structure involves the symmetry of point group C_{3v} rather than that of T_d. In the case of the FeS$_2$-m and CoSb$_2$ type structures the symmetry of the coordination tetrahedron is further reduced and C_{3v} is only an approximation. The environment can, however, be completely defined by the specification of ten parameters, *viz.* four interatomic distances (1 Sb – Sb; 3 Sb – T denoted D_1, D_2, D_3) and six interatomic angles (3 Sb – Sb – T denoted θ_1, θ_2, θ_3; 3 T – Sb – T denoted ϕ_1, ϕ_2, ϕ_3) as evident from Fig. 2. For the compounds with the CoSb$_2$ type

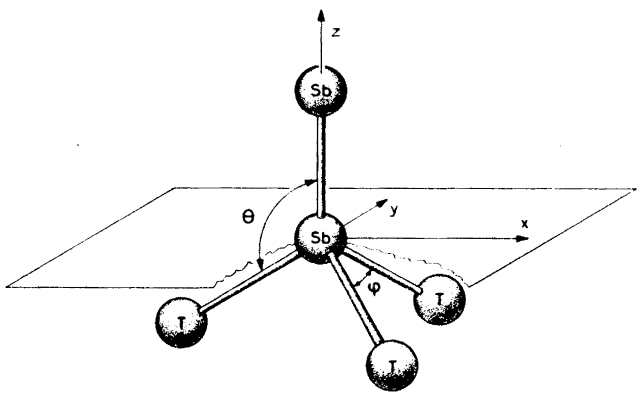

Fig. 2. Model showing a central Sb atom bonded to 1 Sb and 3 T atoms. (The "molecular" symmetry corresponds to C_{3v} in the case of the FeS$_2$-p type structure and to distorted C_{3v} for the FeS$_2$-m type.)

structure the relevant number of such parameters is nineteen as a consequence of the crystallographic non-equivalence of the Sb atoms. The values for these parameters are to be found in Refs. 6, 8, 11, 12.

The bonds between each Sb atom and its 1 Sb and 3 T near neighbours are considered to be of the simple σ type, since there is no evidence for a significant degree of π back-bonding between T and Sb.[2,3] The valence states of the T and Sb atoms are conveniently accounted for in terms of the generalized (8 – N) rule (*cf.*, *e.g.*, Ref. 3). An alternative manner of treatment consists in constructing simplified energy band diagrams by combination of atomic orbitals of matching symmetry on the T and Sb atoms in a representative part of the crystal lattice. The latter approach leads to identical conclusions with regard to the valence situation, but implies an additional feature in permitting a more detailed discussion on the nature of the bonds. Such a hypothetical

bonding scheme has been proposed in Ref. 2, based on the structural characteristics i, ii, and iv (*vide supra*) with the simplifying assumption of a regular octahedral coordination around T. This approximation leads to a model which is adequate in explaining certain features of the crystal structures in terms of the occupancy of the essentially non-bonding d orbitals on T. A more detailed examination of the bonds, however, clearly requires a more refined description of the symmetry of the coordination polyhedra on the basis of the actual atomic arrangements.

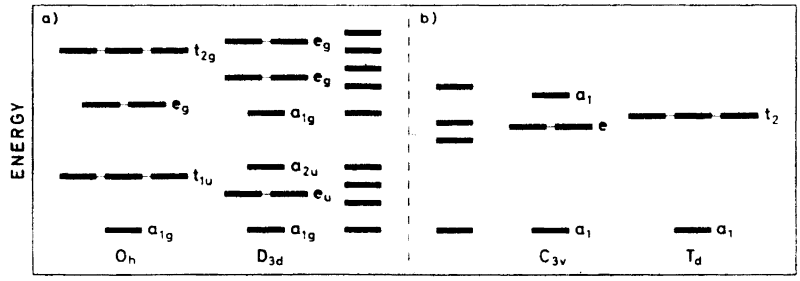

Fig. 3. Schematic energy level diagram for (a) a T atom in the centre of regular and distorted octahedra of 6 X atoms and (b) an X atom in the centre of regular and distorted tetrahedra of 1 X and 3 T atoms. (The number of states in (b) relates to a single X atom.)

Fig. 3 shows a selection of hypothetical energy level diagrams consequent on the distortions of the octahedral and tetrahedral coordinations from the symmetries of O_h and T_d, respectively. The right hand side of the illustration refers to an octahedral polyhedron of 6 X atoms about a central T atom and the left hand side refers to a tetrahedral polyhedron of 1 X and 3 T atoms about an X atom as a centre. On comparing the two sides of the diagram it is apparent that there are differences in the degeneracies of the various energy levels besides the obvious changes in their notations. The extreme cases with O_h and T_d symmetries are both oversimplifications which are incompatible with the crystal structures. A more realistic picture is to be found somewhere in the middle part of Fig. 3, and the following discussion centres around the C_{3v} and distorted C_{3v} symmetries for the Sb atoms.

According to the symmetry of the structure type FeS_2-p, the Sb and T atomic wave functions of the molecular fragment depicted in Fig. 2 transform as described by the irreducible representations of the point group C_{3v}. The molecular orbitals may be envisaged as linear combinations taken over the surrounding Sb and 3 T atoms of s, p, and d atomic wave functions on T and s and p atomic wave functions on Sb. The s and p_z atomic orbitals on Sb transform as a_1 while the p_x and p_y orbitals are of e symmetry (see Fig. 3). The magnitude of the angle θ in Fig. 2 reflects the mixing of the $5p_z$ orbital with the $5s$ contribution. As θ approaches 90° the $5p_x$ and $5p_y$ contributions to the Sb – T bonds increases.

The chemical shift values listed in Table 1 provide further confirmation as to the predominantly covalent bonding in these compounds. According

to the δ values, the total s electron densities at the Sb nuclei for the $T\mathrm{Sb}_2$ compounds are in the region of that for the reference, InSb.

A structural dependence of the δ values is expected to be most clear-cut for the series $\mathrm{CrSb}_2-\mathrm{FeSb}_2-\mathrm{NiSb}_2$ with the FeS_2-m type structure, where one avoids the complication of a variable principal quantum number for the T atoms, which would cause significant differences in $\mathrm{Sb}-T$ overlaps. On this basis, the different bonding characteristics of the T atoms are reflected in the structural data, *e.g.*, in the average $\mathrm{Sb}-\mathrm{Sb}-T$ bond angle θ and the average $\mathrm{Sb}-T$ bond distance D (*cf.* Fig. 2).

The variations of δ with θ and of δ with D are shown in Fig. 4. At first sight it seems impossible to draw any conclusion from this diagram since only three isostructural compounds fulfil the condition of a constant principal quantum number for T. However, the values of θ and D are dictated by the nature of T, and consequently they *must* correlate with δ. The actual form of the functions relating θ, D, and δ is open to examination although the trends in Fig. 4 are consistent with δ being a simple trigonometric function of θ and an inverse function of D.

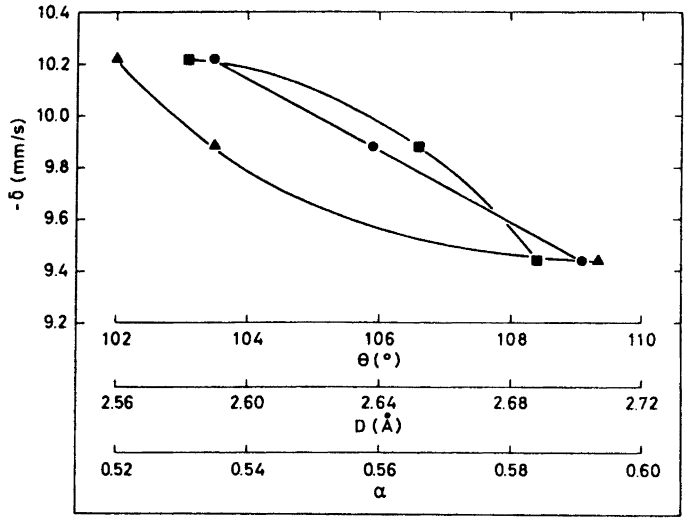

Fig. 4. ^{121}Sb Mössbauer chemical shift for CrSb_2, FeSb_2, and NiSb_2 *versus* α (●), D (■), and θ (▲), respectively. The parameters α, D, and θ are defined in the text.

It is apparent that as θ increases towards the tetrahedral value of 109.47° there is a corresponding decrease in $|\delta|$. This angular dependence implies an increasing Sb $5p_z$ character in the $\mathrm{Sb}-\mathrm{Sb}$ bonds relative to the total $5p_x$, $5p_y$ contributions in the order $\mathrm{CrSb}_2 > \mathrm{FeSb}_2 > \mathrm{NiSb}_2$. Thus, the energy of the molecular orbital originating from the Sb $5p_z$ orbital is lowered relative to those for the molecular orbitals generated by the Sb $5p_x$ and $5p_y$ orbitals. The increase in the $5p_z$ contribution to the $\mathrm{Sb}-\mathrm{Sb}$ bonds, however, does not

necessarily require an enhancement of the *total* 5*p* involvement. Information concerning the latter point is, on the other hand, available from the δ values.

The chemical shift is directly governed by the *s* electron distribution over the one Sb – Sb and three Sb – *T* bonds. Differences in the bonding characteristics of *T* may be assumed to be expressed in terms of the screening of the valence electrons from the nuclei. A measure for this is provided by the effective nuclear charge *Z** as calculated by Slater functions [13] for the relevant atomic orbitals. The *Z** values are used to obtain the "normalized" bond parameters, $\alpha_{A-B} = Z_A^*/(Z_A^* + Z_B^*)$, which reflects the degree of electron delocalization over an A – B bond. The weighted average of the bond parameters α_{Sb-Sb} and α_{Sb-T} for the molecular fragments under discussion are denoted α and plotted against δ in Fig. 4.

The variation of $|\delta|$ with α implies an increase in the net electron delocalization from the Sb $5p_x$ and $5p_y$ atomic orbitals (relative to the 5*s* contribution) into the Sb – *T* bonding orbitals; and, hence, the total *s* electron density at the Sb nucleus increases in the order $CrSb_2 - FeSb_2 - NiSb_2$. Therefore it follows that there is an overall reduction in the energy separation between the molecular orbitals of 5*p* and 5*s* character. This concurs with the fact that *Z** of the atomic 3*d* orbitals of *T* increases in the sequence Cr – Fe – Ni. (The acceptor properties of the $3d_{x^2-y^2}$ and $3d_{z^2}$ atomic orbitals of *T* consequently increase in the same order.)

Although $CoSb_2$ contains a first row transition metal, the presence of the *T* – *T* bonds in its crystal structure prevents a direct comparison with $CrSb_2$, $FeSb_2$, and $NiSb_2$. The most obvious effect of the *T* – *T* bonds is to constrain the bond angle θ. In addition, this structural difference invalidates the basis for a comparison of δ and α. As to the remaining compounds included in Table 1, a comparison of δ in the above manner is complicated by the fact that they do not fulfil the condition of a series of isostructural compounds with an identical principal quantum number for *T*.

In the discussion of the quadrupole splitting values eQV_{zz} for these compounds it should be borne in mind that those with FeS_2-*m* and $CoSb_2$ type structures must have $\eta > 0$. Thus, the constraint $\eta = 0$, as used in the computer fitting of all the experimental spectra, is only strictly valid for the compounds with the FeS_2-*p* type structure where the Sb sites have C_{3v} symmetry. However, it has been shown from simulated spectra [14] that η values less than 0.5 do not have an appreciable effect on the shape of the spectra.

The spectral line-width for $CrSb_2$ at 4.2 K (Fig. 5) is significantly larger than for the other compounds and this behaviour can be attributed to the internal magnetic field at the Sb sites. A pure magnetic hyperfine interaction splits the ground state of ^{121}Sb into six and the excited state into eight levels, giving rise to a total of eighteen allowed transitions. With the additional complexity introduced by the presence of a quadrupole interaction, and given the short life-time of the ^{121}Sb Mössbauer state, the internal magnetic field on Sb in $CrSb_2$ is too weak to produce a resolvable spectrum although the magnetic perturbation is large enough to preclude data reduction for the chemical shift and quadrupole coupling parameters by the computer programme. This finding is in contrast with the observation [15] for MnSb (NiAs type structure) which has an internal field of 353 kOe at 4.2 K [16] originating from a ferro-

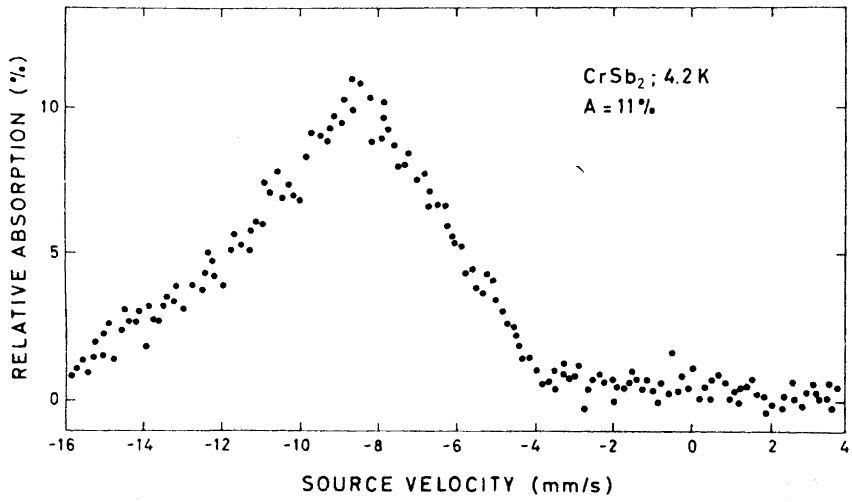

Fig. 5. ^{121}Sb Mössbauer spectrum (at 4.2 K) of $CrSb_2$ in the antiferromagnetic state.

magnetic arrangement [17] of approximately four localized unpaired electrons on the Mn atoms. The lower value for the internal magnetic field in $CrSb_2$ ($< \sim 50$ kOe) is consistent with the fact that there are fewer (two) unpaired electrons per magnetic atom in this compound.[5] An even more important distinction, however, stems from the antiferromagnetic structure, which, in general, gives rise to a relatively small internal magnetic field on the sites of the non-magnetic atoms.

The existence of two non-equivalent Sb sites in $CoSb_2$, $RhSb_2$, and $IrSb_2$ with the $CoSb_2$ type structure does not appear to have manifested itself in increased line-widths. Since this could not be allowed for, it is impossible to determine the influence arising from this source on the values of δ and eQV_{zz}. Certainly, from the structural viewpoint the overall difference between the two Sb sites is relatively small.[8] The Mössbauer parameters for the compounds with the $CoSb_2$ type structure in Table 1 are, for this reason, assumed to be meaningful average representations of the electronic environments of the two Sb sites.

The quadrupole interaction in the compounds with the FeS_2-*p* and FeS_2-*m* type structures arises, for these covalent compounds, mainly from the imbalance in the occupation of the 5*p* orbitals as a result of deviations from cubic electronic symmetry in the environment of the Sb nucleus. To some extent the average distortion from the tetrahedral angle of 109.47° for the bonds around Sb provides a relative measure for this, and Fig. 6 shows a degree of correlation with the observed eQV_{zz} values. Such a correlation is consistent with the bonds in these TSb_2 compounds being predominantly covalent.

Because of the unequal probability of the individual transitions the shape of the absorption envelope yields the sign of eQV_{zz}, which in turn permits a deduction of the sign of the electric field gradient tensor V_{zz}. Since Q for ^{121}Sb is negative, the observed positive eQV_{zz} values give a negative V_{zz} for all the

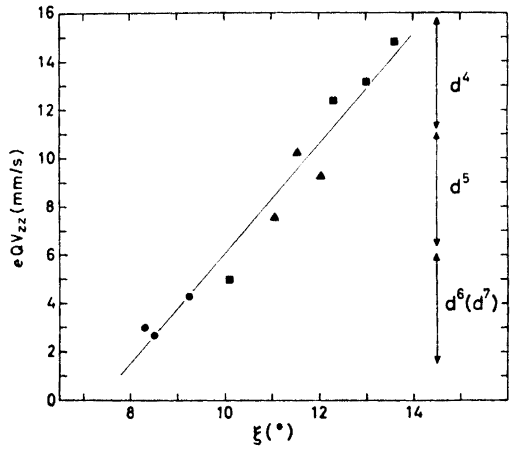

Fig. 6. Average angular distortion (ξ) from T_d symmetry around Sb *versus* quadrupole splitting eQV_{zz} for compounds with the FeS_2-*p* (●), FeS_2-*m* (■), and $CoSb_2$ (▲) type crystal structures. Probable errors are $\pm 0.5°$ in ξ and ± 1 mm/s in eQV_{zz}. The d^i configurations of the metal atoms are indicated on the right hand side of the diagram.

compounds. Because of the C_{3v} symmetry V_{zz} lies along the Sb – Sb bond (or nearly so for the compounds with the FeS_2-*m* and $CoSb_2$ type structures) and the negative sign indicates that the degree of electron delocalization from the Sb $5p_z$ atomic orbital into the relevant a_1 molecular orbital is lower than for the $5p_x$ and $5p_y$ orbitals into the *e* type molecular orbitals. Thus, the electric field gradients at the Sb nuclei are related to the relative energies of the molecular orbitals with $5p$ character. Accepting that the inherent covalency of these compounds strongly reduces the long range lattice contribution, then the electric field gradient may be described by the expression

$$-\tfrac{2}{5}\{2k_1-(k_2+k_3)\}\ \langle r^{-3}\rangle$$

The factors k_1, k_2, and k_3 are inversely proportional to the electronegativities of the molecular orbitals generated from the $5p_z$, $5p_x$, and $5p_y$ atomic orbitals, respectively. (In the case of C_{3v} symmetry $k_2 \equiv k_3$.)

The negative sign of V_{zz} shows that $2k_1 > (k_2+k_3)$ for all the compounds. This, together with the magnitude of eQV_{zz}, suggests that the Sb – Sb bonds have a higher degree of *s* character than the Sb – *T* bonds and that there is a comparatively larger $5p_z$ population relative to the $5p_x$ and $5p_y$ populations localized on the Sb atoms.

Acknowledgement. D.G.N. is grateful to the *Royal Norwegian Council for Scientific and Industrial Research* for the grant of a postdoctorate fellowship.

REFERENCES

1. Brostigen, G. and Kjekshus, A. *Acta Chem. Scand.* **24** (1970) 2983.
2. Brostigen, G. and Kjekshus, A. *Acta Chem. Scand.* **24** (1970) 2993.
3. Kjekshus, A. and Nicholson, D. G. *Acta Chem. Scand.* **25** (1971) 866.

4. Montgomery, H. and Ruby, S. L. *Phys. Rev.* **B 1** (1970) 4529.
5. Holseth, H., Kjekshus, A. and Andresen, A. F. *Acta Chem. Scand.* **24** (1970) 3309.
6. Furuseth, S., Selte, K. and Kjekshus, A. *Acta Chem. Scand.* **19** (1965) 735.
7. Holseth, H. and Kjekshus, A. *Acta Chem. Scand.* **22** (1968) 3273.
8. Kjekshus, A. *Acta Chem. Scand.* **25** (1971) 411.
9. Stevens, J. D. and Ruby, S. L. *Phys. Letters* **A 32** (1970) 91.
10. Stevens, J. G. and Bowen, L. H. *Mössbauer Effect Methodology* **5** (1970) 27.
11. Holseth, H. and Kjekshus, A. *Acta Chem. Scand.* **22** (1968) 3284.
12. Holseth, H. and Kjekshus, A. *Acta Chem. Scand.* **23** (1969) 3043.
13. Slater, J. C. *Phys. Rev.* **36** (1930) 57.
14. Donaldson, J. D., Tricker, M. J. and Dale, B. W. *J. Chem. Soc. Dalton Transactions* **1972** 893.
15. Ruby, S. L. and Kalvius, G. M. *Phys. Rev.* **155** (1967) 353.
16. Tsujimura, A., Hihara, T. and Koi, Y. *J. Phys. Soc. Japan* **19** (1962) 1078.
17. Takei, W. J., Cox, D. E. and Shirane, G. *Phys. Rev.* **129** (1963) 2008.

Received January 28, 1972.